



1 Equatorial deep jets and their influence on the mean
2 equatorial circulation in an idealized ocean model
3 forced by intraseasonal momentum flux convergence

4 Swantje Bastin¹, Martin Claus^{1,2}, Peter Brandt^{1,2}, Richard J. Greatbatch^{1,2}

5 ¹GEOMAR Helmholtz Centre for Ocean Research, Kiel, Germany

6 ²Faculty of Mathematics and Natural Sciences, Kiel University, Kiel, Germany

7 **Key Points:**

- 8 • Equatorial deep jets can be reproduced based on the intraseasonal momentum flux
9 convergence alone
10 • In an idealized ocean model, the deep jets nonlinearly generate mean eastward flow
11 along the equator

Corresponding author: Swantje Bastin, sbastin@geomar.de, sbastin@posteo.de

This article has been accepted for publication and undergone full peer review but has not been through the copyediting, typesetting, pagination and proofreading process which may lead to differences between this version and the Version of Record. Please cite this article as doi: 10.1029/2020GL089111

Abstract

Equatorial deep jets (EDJ) are vertically stacked, downward propagating zonal currents that alternate in direction with depth. In the tropical Atlantic, they have been shown to influence both surface conditions and tracer variability. Despite their importance, the EDJ are absent in most ocean models. Here we show that EDJ can be generated in an idealized ocean model when the model is driven only by the convergence of the meridional flux of intraseasonal zonal momentum diagnosed from a companion model run driven by steady wind forcing, corroborating the recent theory that intraseasonal momentum flux convergence maintains the EDJ. Additionally, the EDJ in our model nonlinearly generate mean zonal currents at intermediate depths that show similarities in structure to the observed circulation in the deep equatorial Atlantic, indicating their importance for simulating the tropical ocean mean state.

Plain Language Summary

In the tropical Atlantic Ocean between 500 m and 2000 m depth, a system of ocean currents called *equatorial deep jets* (EDJ) can be found. This current system consists of multiple currents or *jets* stacked on top of each other and flowing along the equator, alternately (in the vertical) to the east and to the west. The entire system of currents moves slowly downwards, such that at a fixed depth, the flow direction reverses periodically. The EDJ are suggested to influence the weather at the ocean surface, as well as the transport of substances in the deep ocean, for example oxygen that is essential for much of oceanic life. Despite this, their driving mechanisms are not yet fully understood, and they are not yet present in most ocean model simulations.

We show here an idealized ocean model experiment that strongly supports the recently developed theory that the EDJ draw most of their flow energy from the interaction with oceanic equatorial waves with a period of about a month. We also show that, when the EDJ are included in our simulation, a set of mean ocean currents develops that shows similarities to what has been measured in the deep tropical Atlantic Ocean.

1 Introduction

The tropical oceans are characterized by strong zonal current systems. One example are the equatorial deep jets (EDJ) that were first discovered in the Indian Ocean in

the 1970s by Luyten and Swallow (1976). Later, it was found that there are EDJ in all three ocean basins (Hayes & Milburn, 1980; Leetmaa & Spain, 1981; Firing, 1987; Gouriou et al., 1999; Johnson et al., 2002; Johnson & Zhang, 2003). The EDJ take the form of vertically stacked zonal currents along the equator that alternate in direction with depth.

Whereas their vertical wavelength is on the order of a few hundred meters, their zonal structure is coherent over scales comparable to the width of the ocean basins (Gouriou et al., 1999; Johnson & Zhang, 2003; Youngs & Johnson, 2015). Their meridional structure is that of equatorially trapped waves with exponential amplitude decay away from the equator, although there has been some debate about the length scale of this decay which is larger than expected based on inviscid theory (Johnson & Zhang, 2003; Greatbatch et al., 2012). Their vertical scale is thought to be set by the instability, or resonant triad interaction, of intraseasonal waves (Hua et al., 2008) that are, in turn, excited through instabilities in the western boundary currents (d’Orgeville et al., 2007) or in the upper ocean currents (Ascani et al., 2015). Much of the variability at the equator, especially in the Atlantic, is resonant at frequencies corresponding to basin modes (Cane & Moore, 1981; Brandt et al., 2016), which is also true for the EDJ (e.g., d’Orgeville et al., 2007; Ascani et al., 2015; Matthießen et al., 2015, 2017). The period of the gravest of these resonant basin modes, T_n , is set by the time it takes for a Kelvin wave to propagate across the basin, be reflected as the gravest long Rossby wave and propagate back to the western boundary, i.e.

$$T_n = \frac{4L}{c_n} \quad (1)$$

where L is the width of the basin, n is the vertical normal mode in question, and c_n is the gravity wave phase speed for that vertical normal mode. Because of the dependence on the width of the basin, the EDJ in the Pacific vary on considerably longer time scales than those in the Indian or Atlantic Oceans (Youngs & Johnson, 2015). We will focus on the Atlantic EDJ in this article, where, in observations, the EDJ period is approximately 4.5 years (Bunge et al., 2008; Brandt et al., 2011), and their vertical structure is best described by the 15th baroclinic mode (Brandt et al., 2008).

Observations of the Atlantic equatorial deep jets show that their vertical phase propagation is directed downward. Assuming linear wave theory, this implies upward group velocity, i.e. upward energy propagation, also shown in a nonlinear model simulation by

73 Matthießen et al. (2015). Consistent with this, variability at the dominant EDJ period
74 has been found in different surface parameters in the eastern equatorial Atlantic region,
75 including the sea surface temperature, winds, rainfall, and geostrophic surface currents
76 (Brandt et al., 2011). Additionally, the EDJ influence oxygen concentrations in the in-
77 termediate and deep ocean, both the variability and the mean state (Brandt et al., 2012,
78 2015). Finally, the EDJ seem to have an influence on the time mean equatorial circu-
79 lation. Ascani et al. (2015) have shown that there is nonlinear energy transfer between
80 variability at EDJ scales and the mean zonal currents, possibly enhancing the zonal ex-
81 change in the equatorial belt. The presence of zonal currents also strengthens the merid-
82 ional gradients of potential vorticity (Claus et al., 2014), thereby reducing the merid-
83 ional exchange of momentum, tracers and particles (Ménèsquen et al., 2009; Kiko et al.,
84 2017).

85 Despite the EDJs' importance for ocean surface variables and deep ocean tracer
86 distribution and variability, their driving mechanisms are not yet completely understood.
87 Claus et al. (2016) showed that, apart from the excitation of the EDJ by barotropic in-
88 stability of intraseasonal waves, as suggested by Hua et al. (2008), there must also be
89 a mechanism maintaining the EDJ against dissipation directly in their depth range. They
90 argue that given realistic dissipation values, in the absence of forcing, the EDJ energy
91 cannot vertically propagate a much larger distance than the EDJs' vertical wavelength
92 (Claus et al., 2016). A likely mechanism for the EDJ maintenance at depth has recently
93 been proposed by Greatbatch et al. (2018). They showed that there is a positive corre-
94 lation of the slowly varying zonal velocity associated with the EDJ and the convergence
95 of the meridional flux of intraseasonal zonal momentum. The explanation they propose
96 is that the EDJ deform intraseasonal waves such that the convergence of the intrasea-
97 sonal momentum flux becomes nonzero and reinforces the deep jets, comparable to the
98 deformation of eddies in the atmospheric jet stream and the accompanying momentum
99 flux convergence.

100 In this study, we explore the effect of introducing the intraseasonal momentum flux
101 convergence (IMFC) associated with the EDJ, which we diagnose from an idealized, wind-
102 forced model of the tropical Atlantic, as the only momentum forcing into the same model
103 without wind. We can show that it is possible to generate EDJ with realistic amplitude
104 by prescribing the IMFC, corroborating the theory put forward by Greatbatch et al. (2018)
105 that the IMFC likely is the key mechanism responsible for the EDJ maintenance at depth.

106 Additionally we can show that, in our idealized model, the EDJ nonlinearly generate time
107 mean zonal flow in the EDJ depth range, confirming the results of Ascani et al. (2015).

108 The mean zonal circulation that is driven by the EDJ in our model exhibits similarities
109 in structure to the observed mean flow at intermediate depth in the equatorial Atlantic.

110 Section 2 provides a description of the model and our experiment setup. The results are
111 presented in Section 3, and summarized and discussed in Section 4.

112 **2 Model and Methods**

113 **2.1 Model Description and Setup**

114 The results shown in this study have been obtained with an idealized ocean model
115 of the tropical Atlantic basin. We use the Nucleus for European Modelling of the Ocean
116 (NEMO) Version 3.6 (Madec et al., 2017). Our basic setup is inspired by the model se-
117 tups described in Ascani et al. (2015) and Matthießen et al. (2015).

118 Our rectangular model basin with closed boundaries extends from 20°S to 20°N
119 and over a width of 55°, mimicking the width of the Atlantic Ocean at the equator. The
120 basin is 5000 m deep with a flat bottom. The horizontal resolution is $0.25^\circ \times 0.25^\circ$, whereas
121 the vertical resolution is, with 200 levels, considerably finer at depth than that usually
122 employed in ocean models to enable the simulation of EDJ. The vertical mixing scheme
123 is Richardson number dependent, following Pacanowski and Philander (1981). We ini-
124 tialize the model with vertical temperature and salinity profiles from the World Ocean
125 Atlas 2018 (Locarnini et al., 2019; Zweng et al., 2019). For more details see the Support-
126 ing Information.

127 **2.2 Experiment Design**

128 We run this idealized model configuration twice (summarized in Figure 1). For the
129 first run, named Sim-WIND in the following, we force the model at the surface with steady,
130 zonally averaged wind stress calculated from NCEP/NCAR reanalysis data (Kalnay et
131 al., 1996; Kistler et al., 2001). With the wind forcing, both intraseasonal waves and equa-
132 torial deep jets with the same period as found in observations (4.5 years) are present in
133 the model, and the suggested mechanism for maintaining the EDJ through distortion
134 of the intraseasonal waves from Greatbatch et al. (2018) can come into effect (see left
135 panel of Figure 1). From Sim-WIND we diagnose at every grid point in the basin the

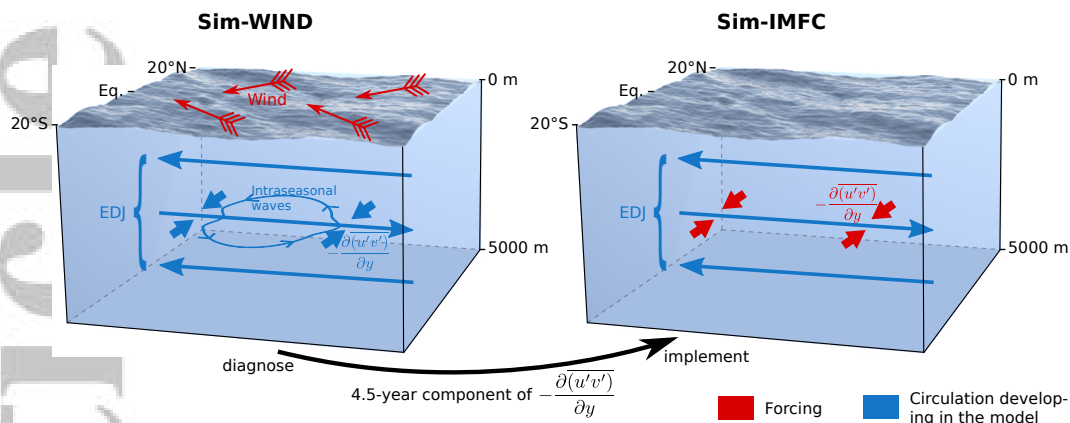


Figure 1. Schematic depiction of the model experiment design.

136 intraseasonal momentum flux convergence (IMFC) that is associated with the EDJ (i.e. the
 137 4.5-year Fourier component of $-\overline{\partial(u'v')/\partial y}$, where the overbar/prime denotes variabil-
 138 ity on time scales larger/smaller than 70 days). The second model run, named Sim-IMFC,
 139 is only forced with the diagnosed IMFC, that is, the term is added to the zonal momen-
 140 tum equation at every time step (see right panel of Figure 1). By adding the term to the
 141 equation rather than applying a relaxation scheme, we ensure that our forcing does not
 142 interfere with other model dynamics.

143 2.3 Argo Analysis

144 We use deep velocity data calculated from Argo float measurements by Lebedev
 145 et al. (2007), covering a time period of nearly 20 years (2000–2019), for an estimation
 146 of the mean zonal flow field at 1000 m depth in the equatorial Atlantic. The Argo data
 147 have been spatially smoothed and corrected for sampling bias associated with the pres-
 148 ence of EDJ before taking the time mean, using methods of Edelson and Krolik (1988),
 149 Lomb (1976), and Scargle (1982). For details see the Supporting Information.

150 3 Results

151 3.1 Generation of EDJ by Intraseasonal Momentum Flux Convergence

152 The characteristics of the EDJ that develop in our idealized model simulations can
 153 be seen in Figure 2. For a comparison of the modeled EDJ to observations the reader
 154 is referred to the Supporting Information; here, it is sufficient to say that the main char-

155 characteristics of the Atlantic EDJ are well represented in our model. The EDJ that emerge
156 through our internal forcing with the intraseasonal momentum flux convergence are very
157 similar to those in the wind-forced simulation, at least between approximately 400 and
158 1800 m depth (below that, the diagnosed IMFC is weak, resulting in weak EDJ in Sim-
159 IMFC). The most striking differences between the simulations are the missing near-surface
160 circulation (e.g. the EUC) due to the lack of wind forcing, and the strong reduction of
161 variability on frequencies other than the EDJ frequency in Sim-IMFC. Both differences
162 are intended and due to our experiment design (recall, in particular, that Sim-IMFC is
163 forced at a single period of 4.5 years). Panels c and d show the time series of zonal ve-
164 locity projected onto the dominant vertical mode. The EDJ in both model simulations
165 have similar amplitudes, although the amplitude shows more fluctuation in Sim-WIND
166 because of the superposition with variability on different time scales. In Panels e and
167 f, amplitude spectra of the zonal velocity, projected onto vertical normal modes, at the
168 center of the model basin are shown. The spectral energy is clearly centered around the
169 gravest equatorial basin mode (cf. Eq. 1 and the solid black line in the figure), and the
170 EDJ (cf. dashed black line) represent a prominent peak.

171 Although the temporal and vertical (and zonal, not shown) structures of the EDJ
172 in both simulations are similar, the meridional structure is different – in Sim-IMFC, the
173 EDJ are significantly narrower than in Sim-WIND. We attribute the difference in EDJ
174 width to the missing influence of the wind and associated variability in Sim-IMFC and
175 the related changes in effective momentum viscosity (cf. Greatbatch et al., 2012), be-
176 cause it is not connected to the structure of the forcing itself. However, this is a topic
177 that requires further research.

178 It was already noted by Greatbatch et al. (2018) that the structure and magnitude
179 of the intraseasonal momentum flux convergence agrees well with the estimates of Claus
180 et al. (2016) regarding the forcing necessary to maintain the EDJ at depth. This is also
181 true for our simulations: The IMFC varying at the EDJ frequency that we diagnosed from
182 Sim-WIND has an amplitude of up to $4 \cdot 10^{-9} \text{ m s}^{-2}$ at the equator, which is consistent
183 with both Claus et al. (2016) and Greatbatch et al. (2018). The fact that this IMFC forc-
184 ing alone can, in our model, drive and maintain EDJ that are reasonably realistic in am-
185 plitude and structure, strongly supports the idea proposed by Greatbatch et al. (2018)
186 based on theoretical considerations that the IMFC is the key process maintaining the
187 EDJ at depth.

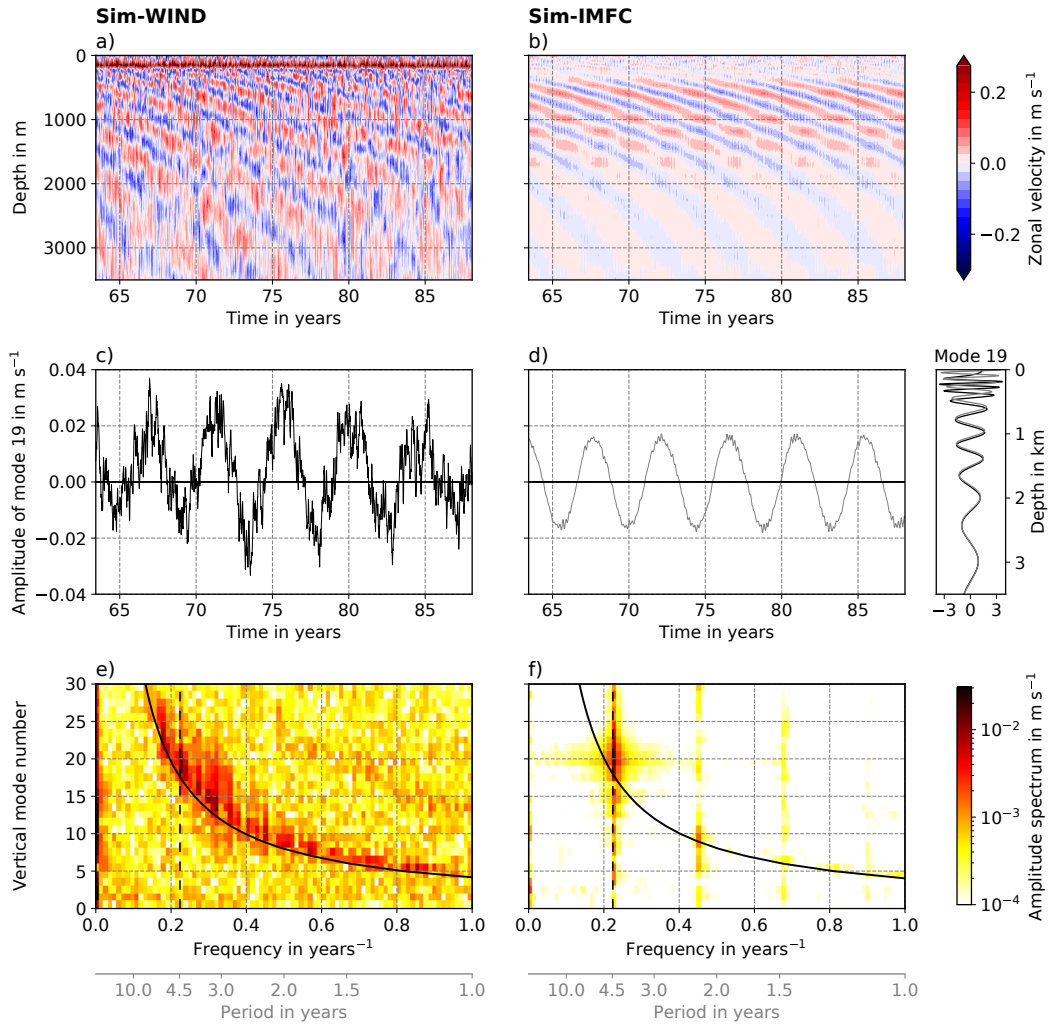


Figure 2. EDJ in the two model runs; Sim-WIND on the left (a, c and e) and Sim-IMFC on the right (b, d and f). Panels a and b show Hovmöller diagrams of zonal velocity on the equator in the center of the model basin. Panels c and d show time series of zonal velocity projected onto the 19th vertical normal mode (one of the dominant modes of the EDJ, cf. Panels e and f) at the center of the basin. The associated structure functions from both model runs are shown on the right. Panels e and f show amplitude spectra of zonal velocity at the center of the basin, calculated after the decomposition of the velocity into vertical normal modes. The gravest equatorial basin mode resonance curve is drawn in solid black. The dashed black line indicates the dominant EDJ frequency.

3.2 Influence on the Time Mean Zonal Flow

As can be seen from Figure 2f, variability on frequencies different from the forcing frequency is generated nonlinearly in Sim-IMFC. Particularly interesting is the generation of time mean zonal flow from the EDJ variability (at the zero frequency in the spectrum). Figure 3a-c shows the time mean zonal velocity at 1000 m depth, from both model runs as well as Argo float data (Lebedev et al., 2007). Note that the color range is scaled by a factor of 5 for Sim-IMFC. In the model, the structure of the mean zonal flow is very similar at all depths where the EDJ are strong, i.e. between approximately 400 and 1800 m. The mean zonal flow at depth in Sim-WIND is dominated by westward flow on the equator and eastward flow approximately 2° north and south of the equator in the western half of the basin. This structure is also found from Argo data in the western basin. The strong westward flow on the equator and the flanking eastward jets at about 2° N/S are usually described as the central part of the equatorial intermediate current system both in the Atlantic and the Pacific Ocean (EICS, cf. e.g. Ascani et al., 2010; Cravatte et al., 2012, 2017; Ménesguen et al., 2019), and have been suggested to originate from dissipation associated with the breaking of downward propagating equatorial Yanai waves by Ascani et al. (2010).

The mean zonal flow that is generated nonlinearly by the EDJ in Sim-IMFC also displays this characteristic structure with one jet on the equator flanked by reversed jets to the north and south; here, however, including a mid-basin change of sign that has also been noted by Ascani et al. (2015). In the western part of the basin between 45° W and about 30° W, the generated mean flow is westward on the equator and eastward to the north and south, whereas in the central and eastern parts of the basin between about 25° W and 5° W there is eastward flow on the equator, flanked by weak westward current bands. The EDJ thus seem to strengthen the equatorial westward and flanking eastward flow that Ascani et al. (2010) attributed to downward propagating Yanai wave beams in the west of the basin, but counteract it in the central and eastern basin.

Interestingly, a similar mid-basin change of current direction can also be seen in the Argo data. The westward flow on the equator only extends into about one third of the basin and is superseded by eastward flow in some regions close to the center of the basin, resembling the structure of the mean zonal flow generated by the EDJ in Sim-IMFC. This suggests that the Atlantic EDJ play a role in establishing the mean zonal current

220 direction on the equator, in the central basin possibly even reversing the otherwise pre-
221 dominantly westward flow that has so far been considered the central branch of the EICS.

222 The magnitude of the flow generated by the EDJ in our model only amounts to at
223 most half of the total time mean zonal velocity measured by Argo around the equator
224 in the center of the basin. This is therefore not enough to explain the Argo mean veloc-
225 ity field. However, it is difficult from our idealized model study to infer the exact mag-
226 nitude of the mean flow that would be generated from the EDJ in the real ocean – for
227 example, the amplitude of the EDJ in our model simulations is rather small (see Fig-
228 ure S5 in the Supporting Information). Because of the nonlinearity of the time mean zonal
229 flow generation, the real Atlantic EDJ might, with a slightly larger amplitude, generate
230 much stronger mean currents. We have tested the effect of different IMFC forcing am-
231 plitudes and thus different EDJ strengths in additional model runs, confirming a larger
232 than linear increase of the mean flow amplitude with linearly increasing EDJ amplitude
233 (shown in the Supporting Information). The structure of the generated mean flow, how-
234 ever, stays the same for different EDJ amplitudes.

235 Figure 3d/e shows the dominant terms of the nonlinear energy transfer from the
236 EDJ to the time mean zonal circulation in Sim-IMFC, averaged over different areas around
237 the equator. Consistent with the results of Ascani et al. (2015), the transfer of energy
238 from EDJ to mean zonal flow mainly occurs through the term $-\partial(\overline{u'u'})/\partial x$, whereas some,
239 but less, energy is transferred from the mean flow to the EDJ through $-\partial(\overline{u'v'})/\partial y$ (the
240 overbar denoting the time mean, the prime deviations from the time mean including mainly
241 the EDJ; not to be confused with the IMFC, where the separation of time scales was be-
242 tween intraseasonal and longer than intraseasonal). The energy transfer is largest close
243 to the equator, but the sign is consistent over almost all averaging areas. The fact that
244 $-\partial(\overline{u'u'})/\partial x$ is the responsible term for the energy transfer from EDJ to mean flow agrees
245 with the zonal structure of the generated mean flow, in particular its mid-basin change
246 of direction.

247 **4 Summary and Discussion**

248 In this study, we have shown that it is possible to drive realistic equatorial deep
249 jets (EDJ) in an idealized ocean model by forcing only with the convergence of the merid-
250 ional flux of intraseasonal zonal momentum that is associated with the EDJ in the mo-

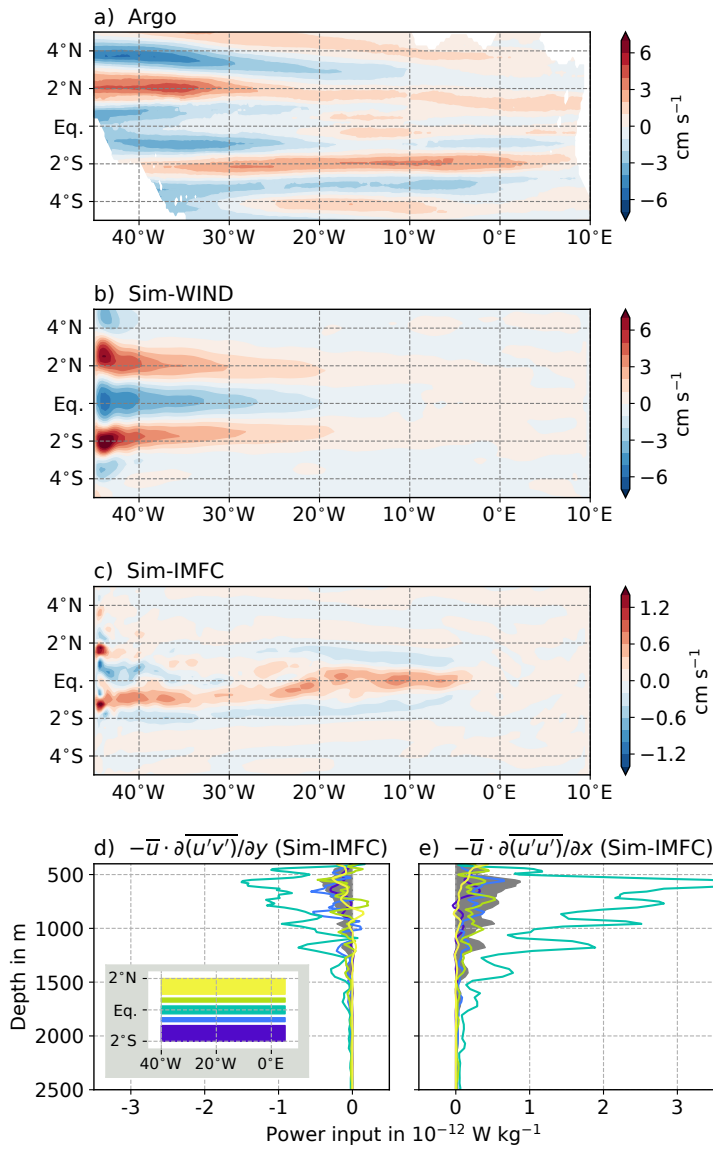


Figure 3. Time mean zonal velocity at 1000 m depth from Argo (Lebedev et al., 2007, Panel a) and from the model runs (Panels b and c). Panels d and e show the time and space averaged nonlinear power input from EDJ into mean zonal flow from Sim-IMFC. The power input through $-\partial(\overline{u'w'})/\partial z$ (not shown) is negligible compared to the other two terms. The overline here denotes a time average, whereas the prime denotes all deviations from this time average (i.e. mainly the EDJ). The inset in Panel d shows the averaging areas corresponding to the color-coded curves in Panels d and e, the filled dark grey curve is the average over all five colored areas.

251 momentum equation. We have also shown that, in our model, the EDJ nonlinearly gener-
252 ate time mean zonal flow that shows similarities in structure to the mean flow measured
253 by Argo floats at 1000 m depth along the equator.

254 The EDJ are stacked zonal jets with large vertical and small zonal wavenumbers
255 in the deep equatorial oceans that propagate downwards with time, the entire system
256 resembling a resonant equatorial basin mode associated with high vertical baroclinic modes.
257 Apart from their excitation mechanisms that have been the topic of research for some
258 time, one interesting feature of the EDJs' dynamics is the question of how they are main-
259 tained against dissipation after their initial generation. Claus et al. (2016) argued that
260 there must be a local forcing process at work in the depth range of the EDJ in order for
261 the EDJ to retain their amplitude over several vertical wavelengths. Greatbatch et al.
262 (2018) suggested that this process could be the deformation of intraseasonal waves by
263 the EDJ, which they argue leads to convergence of the meridional flux of intraseasonal
264 zonal momentum (referred to as intraseasonal momentum flux convergence, IMFC, here),
265 reinforcing the EDJ. As shown by Greatbatch et al. (2018), the magnitude of the IMFC
266 associated with the EDJ agrees well with that of the necessary local forcing amplitude
267 as derived by Claus et al. (2016), making this mechanism a plausible candidate for the
268 EDJ maintenance at depth.

269 With this study, we were able to confirm the theory proposed by Greatbatch et al.
270 (2018) by showing that the IMFC can actually drive sufficiently strong EDJ in an ide-
271 alized ocean model. We diagnosed the IMFC varying at the EDJ frequency from a model
272 configuration that is able to simulate EDJ; a rectangular tropical Atlantic basin model
273 driven by steady wind forcing. Applying the diagnosed IMFC as momentum forcing to
274 a companion model without any other forcing (i.e. without wind) yields EDJ that are
275 very similar in their main characteristics to those arising in the wind-forced model, in
276 particular, they reach a similar amplitude. Our results thus strongly corroborate the the-
277 ory put forward by Greatbatch et al. (2018) that the IMFC is largely responsible for main-
278 taining the EDJ.

279 One thing to bear in mind concerning our modelling approach is that the gener-
280 ation of the EDJ, in reality, does not happen through IMFC as in our simulation. In the
281 real ocean, the momentum forcing through the IMFC only kicks in when the EDJ are
282 already there and strong enough to distort intraseasonal equatorial waves. How the EDJ

283 are generated in the first place is an ongoing topic of research, but it is generally thought
284 that they originate from a number of different mechanisms that involve instabilities in
285 the upper ocean currents and the deep western boundary currents, which excite deep equa-
286 torial intraseasonal variability that rectifies into the EDJ basin modes (e.g., d’Orgeville
287 et al., 2007; Hua et al., 2008; Ascani et al., 2010, 2015; Ménesguen et al., 2019).

288 Interestingly, in the model configuration that we forced only with IMFC varying
289 at the EDJ frequency, variability also on other time scales appears – in particular there
290 is time mean flow that is generated nonlinearly from the EDJ variability. This has al-
291 ready been shown by Ascani et al. (2015) for specific EDJ basin modes, and indeed we
292 can show that in our simulation the energy is transferred from EDJ to mean zonal flow
293 mainly through the zonal self-advection of the EDJ, corroborating their results.

294 The mean zonal flow at intermediate depths that is generated by the EDJ in our
295 model is westward in the western third of the basin, but otherwise predominantly east-
296 ward on the equator, in the opposite direction to the mean westward equatorial flow that
297 has been suggested to be driven by downward propagating, dissipating Yanai wave beams
298 (Ascani et al., 2010) and usually thought to be the central part of the system of low-mode,
299 latitudinally alternating zonal jets in the tropical oceans often called the equatorial in-
300 termediate current system (EICS, e.g. Ascani et al., 2010; Cravatte et al., 2017; Ménesguen
301 et al., 2019). Indeed, Argo observations from 1000 m depth in the Atlantic show that on
302 the equator, the mean zonal velocity is clearly westward only in approximately the west-
303 ern third of the basin and becomes eastward in some places around the basin center. Our
304 results thus suggest that the Atlantic EDJ play a role in establishing the mean zonal cur-
305 rent direction on the equator. However, this effect might be important only in the equa-
306 torial Atlantic Ocean. In the Pacific, the mean zonal flow at intermediate depth appears
307 to be westward throughout most of the basin (e.g. Cravatte et al., 2017), indicating that
308 here, the influence of the EDJ is not strong enough to reverse the current direction. This
309 is consistent with the fact that the Atlantic EDJ are significantly stronger than those
310 in the Pacific and Indian Oceans (e.g. Youngs & Johnson, 2015). It is also consistent with
311 the much larger basin width, i.e. zonal extent of the EDJ, in the Pacific, because the trans-
312 fer of energy to the mean flow depends on the zonal gradient of EDJ strength which is
313 likely small over a larger part of the central Pacific compared to the central Atlantic. East-
314 ward flow along the equator as part of the system of latitudinally alternating zonal jets
315 has also been simulated by Qiu et al. (2013) as the result of nonlinear triad interactions

316 of annual baroclinic Rossby waves. However, it should be noted that they used a $1\frac{1}{2}$ -layer
317 reduced-gravity model designed to simulate the off-equatorial zonal jets, not the equa-
318 torial circulation. Also, the observed westward equatorial flow in the Pacific suggests that
319 the mechanism that is at work in their model is of minor importance directly on the equa-
320 tor.

321 It is known that many global biogeochemical ocean models struggle with oxygen
322 and nutrient distributions in the deep tropical oceans. In general, the oxygen minimum
323 zones in the deep eastern ocean basins are larger in models than in reality, likely because
324 the correct ventilation by the equatorial current system is missing (Dietze & Loeptien,
325 2013; Getzlaff & Dietze, 2013). Associated with this, there is an excess of nutrients in
326 these regions, usually termed “Nutrient Trapping” (Najjar et al., 1992). It has been shown
327 before that the EDJ are responsible for ventilation of the eastern oxygen minimum zones
328 (OMZ), albeit because of the asymmetry in oxygen production and consumption lead-
329 ing to a net eastward oxygen flux due to advection by the EDJ themselves (Brandt et
330 al., 2012). Our results make clear that the Atlantic EDJ likely additionally contribute
331 to OMZ ventilation by generating eastward time mean flow along the equator. The fact
332 that the EDJ are not usually represented in global ocean models thus constitutes a se-
333 rious shortcoming, and we suggest that including them in ocean models could not only
334 lead to a better representation of the variability, but also of the mean state of the equa-
335 torial current system.

336 **Acknowledgments**

337 For more details on model simulations and methods, the reader is referred to the
338 Supporting Information. Scripts and data necessary to obtain the results presented in
339 this paper can be found at <https://doi.org/10.5281/zenodo.3689335> (Bastin et al., 2020).

340 NCEP/NCAR reanalysis data were provided by the NOAA/OAR/ESRL PSD, Boul-
341 der, Colorado, USA, from their web site at <https://www.esrl.noaa.gov/psd/>. Python was
342 used for analysis, Matplotlib (Hunter, 2007) for plotting.

343 This work has been funded in part by the *Sonderforschungsbereich 754 – Climate-*
344 *Biogeochemistry Interactions in the Tropical Ocean*. The authors are not aware of finan-
345 cial conflicts/conflicts of interest related to this work. We thank one anonymous reviewer
346 for their helpful comments.

References

- 347
348 Ascani, F., Firing, E., Dutrieux, P., McCreary, J. P., & Ishida, A. (2010).
349 Deep Equatorial Ocean Circulation Induced by a Forced-Dissipated Yanai
350 Beam. *Journal of Physical Oceanography*, *40*, 1118–1142. doi: 10.1175/
351 2010JPO4356.1
- 352 Ascani, F., Firing, E., McCreary, J. P., Brandt, P., & Greatbatch, R. J. (2015). The
353 Deep Equatorial Ocean Circulation in Wind-Forced Numerical Solutions. *Jour-
354 nal of Physical Oceanography*, *45*, 1709–1734. doi: 10.1175/JPO-D-14-0171.1
- 355 Bastin, S., Claus, M., Brandt, P., & Greatbatch, R. J. (2020). *Supplementary
356 dataset for Bastin et al. (2020), Geophysical Research Letters*. Zenodo. doi:
357 10.5281/zenodo.3689335
- 358 Brandt, P., Bange, H. W., Banyte, D., Dengler, M., Didwischus, S.-H., Fischer, T.,
359 ... Visbeck, M. (2015). On the role of circulation and mixing in the venti-
360 lation of oxygen minimum zones with a focus on the eastern tropical North
361 Atlantic. *Biogeosciences*, *12*, 489–512. doi: 10.5194/bg-12-489-2015
- 362 Brandt, P., Claus, M., Greatbatch, R. J., Kopte, R., Toole, J. M., Johns, W. E.,
363 & Böning, C. W. (2016). Annual and Semiannual Cycle of Equatorial At-
364 lantic Circulation Associated with Basin-Mode Resonance. *Journal of Physical
365 Oceanography*, *46*, 3011–3029. doi: 10.1175/JPO-D-15-0248.1
- 366 Brandt, P., Funk, A., Hormann, V., Dengler, M., Greatbatch, R. J., & Toole, J. M.
367 (2011). Interannual atmospheric variability forced by the deep equatorial
368 Atlantic Ocean. *Nature*, *473*, 497–500. doi: 10.1038/nature10013
- 369 Brandt, P., Greatbatch, R. J., Claus, M., Didwischus, S.-H., Hormann, V., Funk,
370 A., ... Körtzinger, A. (2012). Ventilation of the equatorial Atlantic by the
371 equatorial deep jets. *Journal of Geophysical Research*, *117*, C12015. doi:
372 10.1029/2012JC008118
- 373 Brandt, P., Hormann, V., Bourlès, B., Fischer, J., Schott, F. A., Stramma, L.,
374 & Dengler, M. (2008). Oxygen tongues and zonal currents in the equa-
375 torial Atlantic. *Journal of Geophysical Research*, *113*, C04012. doi:
376 10.1029/2007JC004435
- 377 Bunge, L., Provost, C., Hua, B. L., & Kartavtseff, A. (2008). Variability at In-
378 termediate Depths at the Equator in the Atlantic Ocean in 2000–06: An-
379 nual Cycle, Equatorial Deep Jets, and Intraseasonal Meridional Velocity

- 380 Fluctuations. *Journal of Physical Oceanography*, *38*, 1794–1806. doi:
381 10.1175/2008JPO3781.1
- 382 Cane, M. A., & Moore, D. W. (1981). A Note on Low-Frequency Equatorial Basin
383 Modes. *Journal of Physical Oceanography*, *11*, 1578–1584. doi: 10.1175/1520
384 -0485(1981)011<1578:ANOLFE>2.0.CO;2
- 385 Claus, M., Greatbatch, R. J., & Brandt, P. (2014). Influence of the Barotropic
386 Mean Flow on the Width and the Structure of the Atlantic Equatorial
387 Deep Jets. *Journal of Physical Oceanography*, *44*, 2485–2497. doi:
388 10.1175/JPO-D-14-0056.1
- 389 Claus, M., Greatbatch, R. J., Brandt, P., & Toole, J. M. (2016). Forcing of the
390 Atlantic Equatorial Deep Jets Derived from Observations. *Journal of Physical
391 Oceanography*, *46*, 3549–3562. doi: 10.1175/JPO-D-16-0140.1
- 392 Cravatte, S., Kessler, W. S., & Marin, F. (2012). Intermediate Zonal Jets in the
393 Tropical Pacific Ocean Observed by Argo Floats. *Journal of Physical Oceanog-
394 raphy*, *42*, 1475–1485. doi: 10.1175/JPO-D-11-0206.1
- 395 Cravatte, S., Kestenare, E., Marin, F., Dutrieux, P., & Firing, E. (2017). Subther-
396 moclone and Intermediate Zonal Currents in the Tropical Pacific Ocean: Paths
397 and Vertical Structure. *Journal of Physical Oceanography*, *47*, 2305–2324. doi:
398 10.1175/JPO-D-17-0043.1
- 399 Dietze, H., & Loeptien, U. (2013). Revisiting “nutrient trapping” in global cou-
400 pled biogeochemical ocean circulation models. *Global Biogeochemical Cycles*,
401 *27*, 265–284. doi: 10.1002/gbc.20029
- 402 d’Orgeville, M., Hua, B. L., & Sasaki, H. (2007). Equatorial deep jets triggered by
403 a large vertical scale variability within the western boundary layer. *Journal of
404 Marine Research*, *65*, 1–25. doi: 10.1357/002224007780388720
- 405 Edelson, R. A., & Krolik, J. H. (1988). The discrete correlation function: A new
406 method for analyzing unevenly sampled variability data. *The Astrophysical
407 Journal*, *333*, 646–659. doi: 10.1086/166773
- 408 Firing, E. (1987). Deep zonal currents in the central equatorial Pacific. *Journal of
409 Marine Research*, *45*, 791–812. doi: 10.1357/002224087788327163
- 410 Getzlaff, J., & Dietze, H. (2013). Effects of increased isopycnal diffusivity mim-
411 icking the unresolved equatorial intermediate current system in an earth
412 system climate model. *Geophysical Research Letters*, *40*, 2166–2170. doi:

- 413 10.1002/grl.50419
- 414 Gouriou, Y., Bourlès, B., Mercier, H., & Chuchla, R. (1999). Deep jets in the equa-
415 torial Atlantic Ocean. *Journal of Geophysical Research*, *104*, 21,217–21,226.
416 doi: 10.1029/1999JC900057
- 417 Greatbatch, R. J., Brandt, P., Claus, M., Didwischus, S.-H., & Fu, Y. (2012). On
418 the Width of the Equatorial Deep Jets. *Journal of Physical Oceanography*, *42*,
419 1729–1740. doi: 10.1175/JPO-D-11-0238.1
- 420 Greatbatch, R. J., Claus, M., Brandt, P., Matthießen, J.-D., Tuchen, F. P., Ascani,
421 F., . . . Farrar, J. T. (2018). Evidence for the Maintenance of Slowly Varying
422 Equatorial Currents by Intraseasonal Variability. *Geophysical Research Letters*,
423 *45*, 1923–1929. doi: 10.1002/2017GL076662
- 424 Hayes, S. P., & Milburn, H. B. (1980). On the Vertical Structure of Velocity in the
425 Eastern Equatorial Pacific. *Journal of Physical Oceanography*, *10*, 633–635.
426 doi: 10.1175/1520-0485(1980)010<0633:OTVSOV>2.0.CO;2
- 427 Hua, B. L., d’Orgeville, M., Fruman, M. D., Ménesguen, C., Schopp, R., Klein, P.,
428 & Sasaki, H. (2008). Destabilization of mixed Rossby gravity waves and the
429 formation of equatorial zonal jets. *Journal of Fluid Mechanics*, *610*, 311–341.
430 doi: 10.1017/S0022112008002656
- 431 Hunter, J. D. (2007). Matplotlib: A 2D graphics environment. *Computing in Science
432 & Engineering*, *9*(3), 90–95. doi: 10.1109/MCSE.2007.55
- 433 Johnson, G. C., Kunze, E., McTaggart, K. E., & Moore, D. W. (2002). Tem-
434 poral and Spatial Structure of the Equatorial Deep Jets in the Pacific
435 Ocean. *Journal of Physical Oceanography*, *32*, 3396–3407. doi: 10.1175/
436 1520-0485(2002)032<3396:TASSOT>2.0.CO;2
- 437 Johnson, G. C., & Zhang, D. (2003). Structure of the Atlantic Ocean Equatorial
438 Deep Jets. *Journal of Physical Oceanography*, *33*, 600–609. doi: 10.1175/1520
439 -0485(2003)033<0600:SOTAOE>2.0.CO;2
- 440 Kalnay, E., Kanamitsu, M., Kistler, R., Collins, W., Deaven, D., Gandin, L., . . .
441 Joseph, D. (1996). The NCEP/NCAR 40-Year Reanalysis Project. *Bul-
442 letin of the American Meteorological Society*, *77*, 437–471. doi: 10.1175/
443 1520-0477(1996)077<0437:TNYRP>2.0.CO;2
- 444 Kiko, R., Biastoch, A., Brandt, P., Cravatte, S., Hauss, H., Hummels, R., . . . Stem-
445 mann, L. (2017). Biological and physical influences on marine snowfall at the

- 446 equator. *Nature Geoscience*, *10*, 852–858. doi: 10.1038/NGEO3042
- 447 Kistler, R., Kalnay, E., Collins, W., Saha, S., White, G., Woollen, J., ... Fiorino, M.
448 (2001). The NCEP/NCAR 50-Year Reanalysis: Monthly Means CD-ROM and
449 Documentation. *Bulletin of the American Meteorological Society*, *82*, 247–268.
450 doi: 10.1175/1520-0477(2001)082<0247:TNNYRM>2.3.CO;2
- 451 Lebedev, K. V., Yoshinari, H., Maximenko, N. A., & Hacker, P. W. (2007). YoM-
452 aHa'07: Velocity data assessed from trajectories of Argo floats at parking level
453 and at the sea surface. *IPRC Technical Note No. 4(2)*, 16 p. (updated as of
454 November 2019)
- 455 Leetmaa, A., & Spain, P. F. (1981). Results from a Velocity Transect Along the
456 Equator from 125 to 159°W. *Journal of Physical Oceanography*, *11*, 1030–
457 1033. doi: 10.1175/1520-0485(1981)011<1030:RFAVTA>2.0.CO;2
- 458 Locarnini, R. A., Mishonov, A. V., Baranova, O. K., Boyer, T. P., Zweng, M. M.,
459 Garcia, H. E., ... Smolyar, I. V. (2019). World Ocean Atlas 2018, Volume 1:
460 Temperature. *NOAA Atlas NESDIS*, *81*, 52 pp. (A. Mishonov, Technical Ed.)
- 461 Lomb, N. R. (1976). Least-squares frequency analysis of unequally spaced data. *As-*
462 *trophysics and Space Science*, *39*, 447–462. doi: 10.1007/BF00648343
- 463 Luyten, J. R., & Swallow, J. C. (1976). Equatorial undercurrents. *Deep-Sea Re-*
464 *search*, *23*, 999–1001. doi: 10.1016/0011-7471(76)90830-5
- 465 Madec, G., Bourdallé-Badie, R., Bouttier, P.-A., Bricaud, C., Bruciaferri, D.,
466 Calvert, D., ... Vancoppenolle, M. (2017). NEMO ocean engine.
467 doi: 10.5281/zenodo.3248739
- 468 Matthießen, J.-D., Greatbatch, R. J., Brandt, P., Claus, M., & Didwischus, S.-H.
469 (2015). Influence of the equatorial deep jets on the north equatorial counter-
470 current. *Ocean Dynamics*, *65*, 1095–1102. doi: 10.1007/s10236-015-0855-5
- 471 Matthießen, J.-D., Greatbatch, R. J., Claus, M., Ascani, F., & Brandt, P. (2017).
472 The emergence of equatorial deep jets in an idealised primitive equation model:
473 an interpretation in terms of basin modes. *Ocean Dynamics*, *67*, 1511–1522.
474 doi: 10.1007/s10236-017-1111-y
- 475 Ménesguen, C., Delpéch, A., Marin, F., Cravatte, S., Schopp, F., & Morel, Y.
476 (2019). Observations and Mechanisms for the Formation of Deep Equato-
477 rial and Tropical Circulation. *Earth and Space Science*, *6*, 370–386. doi:
478 10.1029/2018EA000438

- 479 Ménesguen, C., Hua, B. L., Fruman, M. D., & Schopp, R. (2009). Dynamics of the
480 combined extra-equatorial and equatorial deep jets in the Atlantic. *Journal of*
481 *Marine Research*, *67*, 323–346. doi: 10.1357/002224009789954766
- 482 Najjar, R. G., Sarmiento, J. L., & Toggweiler, J. R. (1992). Downward transport
483 and fate of organic matter in the ocean: Simulations with a general circulation
484 model. *Global Biogeochemical Cycles*, *6*, 45–76. doi: 10.1029/91GB02718
- 485 Pacanowski, R. C., & Philander, S. G. H. (1981). Parameterization of Vertical Mix-
486 ing in Numerical Models of Tropical Oceans. *Journal of Physical Oceanogra-*
487 *phy*, *11*, 1443–1451. doi: 10.1175/1520-0485(1981)011<1443:POVMIN>2.0.CO;
488 2
- 489 Qiu, B., Chen, S., & Sasaki, H. (2013). Generation of the North Equatorial Under-
490 current Jets by Triad Baroclinic Rossby Wave Interactions. *Journal of Physical*
491 *Oceanography*, *43*, 2682–2698. doi: 10.1175/JPO-D-13-099.1
- 492 Scargle, J. D. (1982). Studies in astronomical time series analysis. II. Statistical as-
493 pects of spectral analysis of unevenly spaced data. *The Astrophysical Journal*,
494 *263*, 835–853. doi: 10.1086/160554
- 495 Youngs, M. K., & Johnson, G. C. (2015). Basin-Wavelength Equatorial Deep Jet
496 Signals across Three Oceans. *Journal of Physical Oceanography*, *45*, 2134–
497 2148. doi: 10.1175/JPO-D-14-0181.1
- 498 Zweng, M. M., Reagan, J. R., Seidov, D., Boyer, T. P., Locarnini, R. A., Garcia,
499 H. E., ... Smolyar, I. V. (2019). World Ocean Atlas 2018, Volume 2: Salinity.
500 *NOAA Atlas NESDIS*, *82*, 50 pp. (A. Mishonov, Technical Ed.)